Progesterone induces sperm release from oviductal epithelial cells by modifying sperm proteomics, lipidomics and membrane fluidity

Marina Ramal-Sanchez, Nicola Bernabo, Guillaume Tsikis, Marie-Claire Blache, Valérie Labas, Xavier Druart, Pascal Mermillod, Marie Saint-Dizier

HAL Id: hal-03151338
https://hal.inrae.fr/hal-03151338

Submitted on 7 Mar 2022

1 **Title:** Progesterone induces sperm release from oviductal epithelial cells by modifying

2 sperm proteomics, lipidomics and membrane fluidity

3

4 **Authors and affiliations**: Marina Ramal-Sanchez[1,2*], Nicola Bernabo[2], Guillaume

5 Tsikis[1], Marie-Claire Blache[1], Valerie Labas[1,3], Xavier Druart[1], Pascal Mermillod[1],

6 Marie Saint-Dizier[1,4]

7 [1] Physiologie de la Reproduction et des Comportements (PRC) UMR85, INRA, CNRS

8 7247, IFCE, Nouzilly, France

9 [2] Faculty of Bioscience and Technology for Food, Agriculture and Environment,

10 Università degli Studi di Teramo, Italy

11 [3] Plate-forme de Chirurgie et d'Imagerie pour la Recherche et l'Enseignement (CIRE),

12 Pôle d'Analyse et d'Imagerie des Biomolécules (PAIB), INRA, CHRU de Tours,

13 Université de Tours, Nouzilly, France.[1]

14 [4] Université de Tours, Faculté des Sciences et des Techniques, Tours, France

15

[*]**Corresponding author** : Marina Ramal-Sanchez, Università degli Studi di Teramo,

Campus Coste Sant'Agostino, Via R. Balzarini, 1, 64100 Teramo, Italy; Telf : +39 0861

266836, E-mail : mramalsanchez@unite.it

Highlights:

- Spermatozoa released by P4 showed a decreased abundance of Binder of Sperm Proteins (BSP)-3 and -5

- Spermatozoa released by P4 from oviductal cells displayed an increased membrane fluidity

- P4-induced release from oviductal cells modified the sperm lipidomic and proteomic profiles

- A number of interesting proteins and lipids are found as potential sperm fertility biomarkers

Abstract

The sperm reservoir is formed after insemination in mammals, allowing sperm storage in the oviduct until their release. We previously showed that physiological concentrations of progesterone (P4) trigger in vitro the sperm release from bovine oviductal epithelial cells (BOECs), selecting a subpopulation of spermatozoa with a higher fertilizing competence. Here, by using Western-Blot, confocal microscopy and Intact Cell MALDI-TOF-Mass Spectrometry strategies, we elucidated the changes derived by the P4-induced release on sperm cells (BOEC-P4 spz). Our findings show that, compared to controls, BOEC-P4 spz presented a decrease in the abundance of Binder of Sperm Proteins (BSP) -3 and -5, suggesting one mechanism by which spermatozoa may detach from BOECs, and thus triggering the membrane remodeling with an increase of the sperm membrane fluidity. Furthermore, an interesting number of membrane lipids and proteins were differentially abundant in BOEC-P4 spz compared with controls.

Keywords: progesterone, sperm capacitation, Binder of Sperm Proteins, oviduct, proteomics, lipidomics

1. Introduction

In mammals, after mating or artificial insemination, only a few spermatozoa reach the oviduct, where they bind to the luminal epithelial cells for hours to days forming the so called "functional sperm reservoir" (Hunter and Wilmut, 1984). During this storage, the interactions between the oviductal epithelial cells (OEC) and spermatozoa are believed to play an important role in sperm selection (Mburu et al., 1997; Tienthai, 2015) maintenance of sperm viability (Ellington et al., 1999) and prevention of premature capacitation (Murray and Smith, 1997) before ovulation. Then, around the time of ovulation, spermatozoa are released from the OEC and move towards the fertilization site (Coy et al., 2012). The exact mechanism by which sperm detach from the oviductal epithelium and become able to fertilize the oocyte in vivo is not fully understood. However, the ovarian steroid hormone progesterone (P4) has been proposed as a major regulator of sperm release in birds (Ito et al., 2011) and pigs (Hunter, 2012). We reported a consistent increase in intra-oviductal P4 concentrations (on average from 6 ng/mL before ovulation to 57 ng/mL after ovulation) in bovine oviducts ipsilateral to the side of ovulation (Lamy et al., 2016). Previous in vivo studies in pigs demonstrated that an injection of P4 into the oviductal wall or directly into the sperm reservoir induced the sperm release together with an increase in the polyspermy rates (Hunter, 2008). Thanks to an in vitro model consisting of monolayers of bovine OECs (BOECs) from the whole oviduct, we showed in an earlier study that P4 at concentrations of 10 and 100 ng/mL was an inductor of sperm release from BOECs (Lamy et al., 2017), a result recently confirmed by other researchers (Romero-Aguirregomezcorta et al., 2019). Furthermore, spermatozoa bound to BOECs and then released from BOECs by P4 action showed higher fertilizing ability compared with the control group (Lamy et al., 2017). However, the exact changes induced by the binding to BOECs and

67 subsequent P4-induced release from these cells on sperm physiology remain to be

68 elucidated.

69   P4 was found to stimulate mammalian sperm capacitation, hyperactivated

70 motility, acrosome reaction and chemoattraction at various doses (Gimeno-Martos et al.,

71 2017; Teves et al., 2006). In addition, three proteins from the seminal plasma that bind

72 to the bovine sperm surface at the time of ejaculation have been identified as involved

73 in sperm binding to OECs: Binder of Sperm Protein 1 (BSP-1, also called PDC-109 or

74 BSP-A1/A2), BSP-3 (or BSP-A3), and BSP-5 (or BSP-30KDa) (Gwathmey et al., 2006,

75 2003). BSPs have been reported to play important roles along the female genital tract in

76 sperm membrane stabilization and prevention of premature capacitation (Plante et al.,

77 2016a). Furthermore, the removal of BSPs from the sperm surface by oviductal

78 components is considered as the initial step promoting cholesterol and phospholipids

79 efflux, leading to an increase in membrane fluidity, sperm capacitation and eventually

80 acrosome reaction (Thérien et al., 1999, 1998).

81   Thus, the aim of this study was to investigate the mechanisms involved in the

82 release of spermatozoa from the sperm reservoir using our in vitro model. Based on the

83 key role played by BSPs on sperm-BOECs binding, we first evaluated the abundance of

84 BSPs on spermatozoa bound to BOECs and then released by P4 compared with

85 unbound spermatozoa or control spermatozoa treated or not with P4. The changes in

86 membrane fluidity, a marker of sperm capacitation, was then investigated in the various

87 experimental groups. Last, changes induced by P4 in sperm proteins and lipids during

88 the releasing process were explored using mass spectrometry on intact sperm cells.

89 **2. Materials and methods**

90   Unless otherwise stated, all chemicals were purchased from Merck-Sigma-

91 Aldrich (Saint Quentin-Fallavier, France). Bovine oviducts were obtained from a

92 commercial slaughterhouse and bovine semen from a breeding cooperative; no

93 experiments on live animals were performed. The experiments performed are in

94 accordance with the EU Directive 2010/63/UE.

95   **2.1. Co-incubation of bovine spermatozoa with BOECs**

96   A pool of frozen semen from three bulls (*Bos Taurus*, 0.25-mL straws,

97 approximately 20×10^6 spermatozoa/straw) was used in all the experiments. Straws were

98 thawed in a water bath at 37°C for one minute and then motile spermatozoa were

99 selected through a Percoll (GE Healthcare Life Sciences, Velizy-Villacoublay, France)

100 density gradient (90-45%). The sperm pellet was rinsed in 10 mL of STL-medium

101 (Tyrode medium supplemented with 25 mM Bicarbonate, 10 mM Lactate, 100 IU/mL

102 Penicillin, 100 µg/mL Streptomycin and 2.4 mg/mL HEPES) and then centrifuged at

103 100 g for 10 min. Sperm motility was visually estimated by light microscopy before

104 each experiment and only samples with a sperm motility >90% were considered in

105 further analyses.

106   Oviductal epithelial cells were collected from scratching the whole oviduct inner

107 surface and used as confluent monolayers, as previously described (Lamy et al., 2017)

108 with slight modifications. Preliminary experiments showed no difference between fresh

109 and frozen-thawed BOECs in terms of viability, time to reach confluency, morphology,

110 sperm binding and release under P4 action (data not shown). For the present study,

111 different pools of frozen-thawed BOECs were used in the various experiments. Briefly,

112 both oviducts from 5-7 adult cows at peri-ovulatory stages were collected at a

113 slaughterhouse and transported to the laboratory within 2 hours after the death of the

114   animals. Only oviducts in the pre-ovulatory (presence of a pre-ovulatory follicle and

115   one corpus albicans) and post-ovulatory (red recently ovulated corpus luteum, no

116   follicle >10 mm in diameter) stages were used, as previously described (Lamy et al.,

117   2016). The process of primary oviductal cell culture used in the present study has been

118   described and validated by our group (Mermillod et al., 1993; Van Langendonckt et al.,

119   1995). After dissection, BOECs were gathered by scratching the whole oviducts

120   (ampulla and isthmus tracts), pooled and then rinsed three times in a washing medium

121   (TCM 199 supplemented with Gentamicin 10 mg/mL and BSA 0.2%). BOECs were

122   then diluted 1:10 in a freezing medium (TCM 199 supplemented with DMSO 10%,

123   Gentamicin 80 µg/mL and FBS 10%), aliquoted in cryotubes before being placed

124   overnight at − 80ºC and then stored in liquid nitrogen. For each experiment, an aliquot

125   of BOECs was thawed in a water bath at 34ºC, then transferred into a thawing-washing

126   medium (TCM 199 with FBS 10% and Gentamicin 80 µg/mL), washed twice and

127   cultured in 12 well plates (TCM 199 with FBS 10% and Gentamicin 80 µg/mL). Once

128   reached the confluence (after 6-7 days of culture), BOECs were washed twice with IVF

129   medium (Tyrode medium supplemented with 25 mM bicarbonate, 10 mM lactate, 1 mM

130   pyruvate, 6 mg/mL fatty acid free BSA, 100 IU/mL penicillin and 100 µg/mL

131   streptomycin) and bovine spermatozoa were added to the cells at a final concentration

132   of 4×10^6 sperm cells/mL in the same IVF medium and under culture conditions

133   (humidified atmosphere, 5% CO_2, 38.8 °C). After 30 min of co-incubation with BOECs,

134   unbound and slightly attached spermatozoa (BOEC group) were collected by aspiration

135   of the supernatant and two additional washings with IVF medium. The release of bound

136   spermatozoa from BOECs was then induced by adding P4 (100 ng/mL) to the culture

137   medium for 1 h. According to P4 concentrations previously measured in the bovine

138   oviductal fluid at the postovulatory period (Lamy et al., 2016), a P4 concentration of

139   100 ng/mL was considered to be physiological. The P4 solution was diluted in absolute

140   ethanol and added at a final concentration of 0.5% ethanol in the culture medium.

141   Preliminary experiments in our laboratory showed that vehicle controls containing an

142   equivalent amount of ethanol had no effect on the time course of sperm binding and

143   release (data not shown). Furthermore, ethanol at low concentrations (0.1-1%) was

144   shown to have no detectable effect on sperm motility, viability, capacitation, cholesterol

145   efflux and acrosome reaction during up to 6 h of incubation (Lukacova et al., 2015;

146   Therien and Manjunath, 2003). Spermatozoa released from BOECs by P4 action

147   (BOEC-P4 group) were collected by washing three times with IVF medium. Two

148   control groups of spermatozoa at the same sperm concentration were run in parallel in

149   each experiment. Control groups were incubated in the IVF medium, centrifuged the

150   same time and manipulated the same way (including pipetting) than the treated BOEC-

151   P4 group. One control group was similarly manipulated but not incubated with BOECs

152   nor P4 (CTRL group). Another group of spermatozoa was incubated without BOECs for

153   30 min in the IVF medium and then P4 (100 ng/mL) was added to the culture medium

154   for 1 h (P4 group), i.e., at the same dose and incubation time than the BOEC-P4 group.

155   It was not possible to constitute a control group in which P4 was replaced by vehicle

156   after BOEC incubation and elimination of unbound sperm because 1h of incubation

157   with ethanol at 0.5% did not induce sperm release from BOEC.

158   **2.2. Evaluation by Western blot of BSP abundance in spermatozoa**

159   Previous studies using the same in vitro system showed that only sperm heads

160   with intact acrosome did bind to the surface of BOECs (Lamy et al., 2017). In order to

161   reject the hypothesis whereby the release of bound spermatozoa by P4 was due to the

162   loss of their acrosome, the integrity of acrosomes in the BOEC-P4 and CTRL groups

163   was evaluated using a double staining with PNA (Peanut Agglutinin lectin) and Hoechst

164   33342 followed by examination under confocal microscopy. Acrosomes were found to

165   be intact in more than 90% of spermatozoa in both groups (data not shown). For

166   Western-Blot analyses, spermatozoa from all the experimental groups were collected

167   and immediately washed twice in PBS and centrifuged at 2000 g for 3 min before

168   protein extraction. Samples were then diluted in lysis buffer (2% SDS in 10 mM Tris,

169   pH 6.8) with a protease inhibitor cocktail and centrifuged (15,000 g for 10 min, 4ºC) to

170   separate the protein-rich supernatant from the cellular debris. The concentration in

171   proteins was assessed in sperm supernatants using the Uptima BC Assay kit (Interchim,

172   Montluçon, France) before dilution in loading buffer (Laemmli buffer 5×) and heating

173   (90ºC for 5 min). Sperm samples extracts were migrated (10 µg of proteins per lane) on

174   a SDS-PAGE 4-15% gradient gel (Mini-PROTEAN® TGX™ Precast Protein Gels,

175   BioRad) and blotted on a nitrocellulose membrane using the Trans-Blot® TurboTM

176   Transfer System (BioRad, Marnes-la-Coquette, France). The membranes were stained

177   with Ponceau S solution (5 min at room temperature, gentle shaking) and scanned with

178   Image Scanner (Amersham Biosciences, GE Healthcare Life Sciences) to check the

179   homogeneous loading among lanes and for normalization (see below). Membranes were

180   blocked in 5% (w/v) milk powder diluted in TBS-T (Tris-buffered saline with 1% (v/v)

181   Tween 20) for 1 h and then incubated with the primary antibody diluted at 1:1000

182   (gentle shaking, 4ºC, overnight). Anti-sera against purified bovine BSP-1, BSP-3 and

183   BSP-5 proteins were kindly provided by Dr. Manjunath (Department of Biochemistry

184   and Medicine, University of Montreal) and antibodies were purified with the Melon Gel

185   IgG spin purification kit (Thermo Fisher Scientific, City, Country), following the

186   supplier's instructions. Blots were finally incubated with fluorescent secondary

187   antibody IRDye® 800CW anti-Rabbit IgG (gently shaking, 37ºC, darkness, 45 min)

188   diluted at 1:10,000 before revelation with infrared scanner Odyssey® CLx (LI-COR

189   Biotechnology, Lincoln, USA). Protein signals were analyzed by Image Studio™

190   software (LI-COR Biotechnology, Lincoln, USA). The bands were quantified

191   afterwards using ImageQuantTL (GE Healthcare LifeSciences). Three biological

192   replicates were performed for each antibody and each condition. To normalize the data,

193   Ponceau S staining was used, as previously described (Romero-Calvo et al., 2010).

194   Briefly, the whole lanes were quantified by densitometry using the TotalLab Quant

195   software (version 11.4,TotalLab, Newcastle upon Tyne, UK). Then the experimental

196   groups (BOEC, BOEC-P4 and P4) were normalized with the CTRL group.

197   **2.3. Evaluation of sperm membrane fluidity by fluorescence recovery after**

198   **photobleaching (FRAP) analysis**

199   Due to the need of analyzing live spermatozoa in a very short length of time,

200   only CTRL-spz and BOEC-P4 groups, which displayed the most contrasted profiles in

201   BSP abundance, were analysed. FRAP experiments were performed as previously

202   described (Bernabò et al., 2017) with some modifications. Briefly, the lipophilic

203   fluorescent molecule DilC12(3) perchlorate (ENZ-52206, Enzo Life Sciences, USA)

204   was added (1:1000) for the last 15 min of the sperm-BOECs co-incubations.

205   Spermatozoa were then collected and FRAP was carried out within 60 min after

206   collection with a laser-scanning confocal microscope LSM780 (Zeiss, Oberkochen,

207   Germany) with the following acquisition parameters: Plan Apo 63X oil objective,

208   numerical aperture 1.4; zoom 4.2; 1 airy unit; 1 picture every 0.230 sec; fluorescence

209   bleaching and recovery performed at $\lambda exc = 561$ nm and $\lambda em = 595$ nm with one scan

210   for basal fluorescence record at 2.4% of the maximum laser power, one scan at 100%

211   laser power for bleaching, and 25 scans for monitoring recovery at 2.4% of the

212   maximum laser power. Recovery curves were obtained and analysed using the

213   simFRAP plug-in for Fiji ImageJ (https://imagej.nih.gov/ij/plugins/sim-frap/index.html,

214   01/27/2019) (Blumenthal et al., 2015). The parameters set were the following: pixel size

215   0.109 µm; acquisition time per frame 0.095 sec. The results are expressed as diffusion

216   coefficient (cm^2/sec). Six independent experiments were carried out, with an average of

217   15 spermatozoa analysed per condition and per replicate.

218   **2.4. Statistical analysis of Western-blot and FRAP data**

219   For statistical analysis, GraphPad Prism 6 Software (La Jolla, CA, USA) was

220   used. All data were first subjected to normality test (Agostino-Pearson and Shapiro-

221   Wilcoxon tests). As Western-blot and FRAP data did not follow a normal distribution,

222   differences between the groups were analyzed by Kruskal-Wallis' tests followed by

223   Dunn's multiple comparisons tests for Western-blot and Mann-Whitney U test for

224   FRAP analysis. Differences were considered statistically significant when p<0.05.

225   **2.5. Sperm proteomic and lipidomic profiling by Intact Cell MALDI-TOF Mass**

226   **Spectrometry (ICM-MS)**

227   For proteomic and lipidomic analyses, all groups of spermatozoa were washed

228   three times in Tris-Sucrose Buffer (TSB, 20 mM Tris-HCl, 260 mM sucrose, pH 6.8) to

229   remove the culture media and salts. For proteomic profiling, 0.5 µL of saturated CHCA

230   (α-cyano-4-hydroxycinnamic acid) matrix dissolved in 100% ethanol was spotted on a

231   MALDI plate (MTP 384 polished steel) and dried (30 min, room temperature) before

232   adding 10^5 spermatozoa (determined using a Thoma cell counting chamber) in one µl,

233   then 2.5 µL of saturated CHCA (α-cyano-4-hydroxycinnamic acid) matrix dissolved in

234   50% acetonitrile/50% water (v/v) in presence of 0.3% TFA (trifluoroacetic acid) was

235   added. For lipidomic profiling, 2×10^5 spermatozoa in 0.5 µL were spotted and overlaid

236   with 2 µL of DHAP (2,5-dihydroxyacetophenone) matrix at 20 mg/mL solubilized in

237   90% methanol/10% in presence of 2% TFA. For each condition, three biological

238 replicates were performed and for each biological replicate, twenty technical replicates

239 were spotted.

240 Spectra were acquired using a Bruker UltrafleXtreme MALDI-TOF instrument (Bruker

241 Daltonics, Bremen, Germany) equipped with a Smartbeam laser at 2 kHz laser

242 repetition rate following an automated method controlled by FlexControl 3.0 software

243 (Bruker Daltonics, Bremen, Germany). Spectra were obtained in positive linear ion

244 mode in the 1,000–30,000 m/z (mass/charge) range for proteomics and 100-1,800 m/z

245 range for lipidomics. Each spot was analyzed in triplicate. After external calibration,

246 each spectrum was collected as a sum of 1,000 laser shots in five shot steps (total of

247 5,000 spectra) with a laser parameter set at medium. To increase mass accuracy (mass

248 error <0.05%), an internal calibration was performed on a mix of cells and calibrant

249 solution (for proteomic, 1µL of calibrant solution containing Glu1-fibrinopeptide B,

250 ACTH (fragment18-39), insulin and ubiquitin, cytochrome C, myoglobin and

251 trypsinogen, while for lipidomic, 1 µL of calibrant solution containing Caffein, MRFA

252 peptide, Leu-Enkephalin, Bradykinine 2–9, Glu1-fibrinopeptide B; reserpine;

253 Bradykinine; Angiotensine I). A lock mass correction was applied to one peak with high

254 peak intensity in all spectra using flexAnalysis 4.0 software (Bruker). For proteomics,

255 the peak at m/z 6821.46 was selected, while for lipidomics, the calibration was achieved

256 with the mass corresponding to the phosphatidylcholine 34:1 (PC 34:1; $[M+H]^+$:

257 760.5856 m/z).

258 **2.6. Quantification and statistical analysis of ICM-MS data**

259 Spectral processing and analysis were performed with ClinProTools v3.0

260 software (Bruker Daltonics, Bremen, Germany). The data analysis began with an

261 automated raw data pre-treatment workflow, comprising baseline subtraction (Top Hat,

262   10% minimum baseline width) and two smoothings using the Savitzky-Golay

263   algorithm. The spectra realignment was performed using prominent peaks (maximal

264   peak shift 2000 ppm, 30% of peaks matching most prominent peaks, exclusion of

265   spectra that could not be recalibrated). Normalization of peak intensity was performed

266   using the Total Ionic Count (TIC) in order to display and compare all spectra on the

267   same scale. Automatic peak detection was applied to the total average spectrum with a

268   signal/background noise greater than 2.

269   The intra- and inter-experiment variability in measurements were evaluated by a

270   coefficient of variation (CV). For CTRL, BOEC, BOEC-P4 and P4 groups, mean CV

271   values did not exceed 18.4%, 21.2%, 23.1% and 20% for proteomics, and 31.3%,

272   34.5%, 34.5% and 36.1% for lipidomics, respectively. Differential analyses between

273   groups (N = 180-200 MALDI spectra per group) were performed using the non-

274   parametric Kruskal-Wallis and Wilcoxon tests for multiple and paired comparisons,

275   respectively. Fold Change (FC) was calculated as the ratio between the mean

276   normalized intensity values. Masses were considered statistically differential between

277   groups if the p-value was < 0.01 with a FC > 1.5 or < 0.67. Receiver operating

278   characteristic (ROC) curves were generated and only masses with areas under the curve

279   (AUCs) > 0.8 were retained. Principal component analysis (PCA) and hierarchical

280   clustering were performed on differential masses using the RStudio Software (RStudio,

281   Boston, MA, USA) (installed packages: *readr, robustbase, caTools, RColorBrewer,*

282   *MALDIquantForeign, FactoMineR, gplots*).

283   **2.7. ICM-MS data processing for lipid and protein identification**

284   In order to identify the lipids corresponding to the differential peaks obtained by ICM-

285   MS profiling, the masses observed were confronted to a local database created from

286   previous analyses of bovine follicular cells and biological fluids. This database is a

287   merged list of lipids identified by high resolution mass spectrometry (HRMS) using

288   liquid chromatography coupled with mass spectrometry (LC-MS) and direct infusion

289   for MS/MS structural analyses, as recently described (Bertevello et al., 2018). The

290   comparison of the masses observed by ICM-MS and the monoisotopic masses identified

291   by HRMS was performed with a max mass tolerance of 0.1 Da for lipids.

292   In order to identify the proteins corresponding to the differential peaks obtained by

293   ICM-MS profiling, a local database from a previous analysis of ovine spermatozoa by

294   HRMS coupled to µLC was used. In this analysis, 1 mg of the peptides/proteins was

295   subjected to various fractionations through reversed phase and gel filtration

296   chromatographic separations, as previously described (Soler et al., 2016). All the data

297   acquired by µLC-MS/MS were automatically processed by the ProSight PC software

298   v4.0 (Thermo Fisher, San Jose, California, USA) (Soler et al., 2016). All the data files

299   (*.raw) were processed using the cRAWler application. Molecular weights of precursor

300   and product ions were determined using the xtract algorithm. Automated searches were

301   performed on PUF files using the "Biomarker" search option against a database made

302   from the UniprotKB Swiss-Prot Ovis aries release

303   ovis_aries_2017_07_top_down_complex (28256 sequences, 512072 proteoforms)

304   downloaded from http://proteinaceous.net/database-warehouse/. Iterative search tree

305   was designed for monoisotopic precursors and average precursors at 25 ppm and 2 Da

306   mass tolerance, respectively, and both at 15 ppm for fragment ion level. For all

307   searches, the N-terminal post-translation modifications were considered. Then, all the

308   *.puf files were additionally searched in "Absolute mass" mode using 1000 Da for

309   precursor search window. For identification of endogenous biomolecules, we validated

310   automatically all the peptidoforms/proteoforms with E value $<1E^{-8}$. Furthermore, we

311 validated all hits presenting a C score > 3 (LeDuc et al., 2014). The comparison of the

312 masses observed by ICM-MS and the average masses identified by Top-Down was

313 performed with a max mass tolerance of 0.05% for proteins.

314 In TD results list, the entry names and gene names were recovered from the UniProtKB

315 accession numbers from *Ovis aries* annotated proteins using the Retrieve/ID mapping of

316 Uniprot (http://www.uniprot.org/uploadlists/) and listed. Proteins identified in *Ovis*

317 were mapped to the corresponding *Bos taurus* taxon by identifying the reciprocal-best-

318 BLAST hits using blastp resource (http://blast.ncbi.nlm.nih.gov/Blast.cgi). Only protein

319 sequences with 100% identity and 100% query cover were retained. The gene name and

320 accession number of identified proteins were recovered from the NCBI database.

321 Protein functions and cellular location were recovered from UniProtKB (Swiss-prot)

322 (https://www.uniprot.org/uniprot/, 01/27/2019) Last, the potential role of proteins

323 identified in membrane lipid rafts was assessed using the RaftProt Database V2

324 (Mammalian Lipid Raft Proteome Database, http://raftprot.org/, 01/27/2019) by

325 downloading the list of lipid-raft associated proteins detected in bovine experiments

326 (evidence based on Gene Name and UniprotID).

327 **3. Results**

328 **3.1. Binding to BOECs and subsequent P4-induced release decreased the**

329 **abundance of BSPs on sperm and increased sperm membrane fluidity**

330 Spermatozoa treated with P4 alone (P4 group) and spermatozoa unbound after

331 incubation with BOECs (BOEC group) did not display any change in BSP abundance

332 compared with controls (CTRL group). By contrast, a significant decrease in the

333 abundance of BSP-3 and BSP-5 was evidenced on spermatozoa bound to BOECs and

334 then released by P4 (BOEC-P4 group) compared with CTRL (fold changes of

335 normalized values of 2.89 and 2.76 for BSP-3 and BSP-5, $p < 0.05$ and $p < 0.01$,

336 respectively), while the abundance of BSP-1 tended to decrease (fold change of 2.16, p

337 > 0.05) (Fig. 1). In addition, FRAP analyses evidenced an increase in membrane fluidity

338 in BOEC-P4 sperm cells compared with the CTRL group ($p < 0.05$) (Fig. 2).

339 **3.2. Binding to BOECs and subsequent P4-induced release changed sperm**

340 **lipidomic profiles**

341 A total of 206 lipid molecular species with a mass range between 400 and 1000 Da were

342 detected among experimental groups. Of those, 123 masses were differential when

343 considering all possible paired comparisons between the four experimental groups (Fig.

344 3A). The action of P4 alone did not induce any significant change in sperm lipid

345 composition compared with the control group (P4 vs. CTRL). By contrast, spermatozoa

346 bound to BOECs and then released by P4 (BOEC-P4) showed 116 and 34 differential

347 masses compared with spermatozoa treated by P4 alone (P4) and those just manipulated

348 (CTRL), respectively. In addition, the incubation with BOECs without binding (BOEC

349 group) induced 33 differential masses as compared with CTRL, among which a high

350 proportion (29/33) was already identified in the BOEC-P4 vs. CTRL comparison (Fig.

351 3A). The hierarchical clustering of differentially abundant lipid masses evidenced a

352 closeness in lipid profiles between the BOEC-P4 and BOEC groups compared with the

353 CTRL and P4 groups (Fig. 4A).

354 **3.3. Identification of differentially abundant lipids**

355 A total of 84 lipids, listed in Supplementary Table 1, could be annotated. Most of those

356 were phosphatidylcholines (PC) (35/84), among which the PC(36:2) at *m/z* 786.6 and

357 PC(36:1) at *m/z* 788.6 exhibited the highest fold changes between conditions (see

358 Supplementary Table 1 for all paired-wise ratios between normalized values). A high

359   proportion of sphingomyelins (SM) (14/84) was also identified, followed by

360   lysophosphatidylcholines (LPC) (9/84). The remaining masses identified were

361   cholesteryl esters (CE), fatty acyl carnitines (CAR), ceramides (Cer), diacylglycerols

362   (DAG), lysophosphatidylethanolamines (LPE), phosphatidylethanolamines (PE) and

363   triacylglycerols (TAG). A detailed classification of the lipids identified in this analysis

364   and their corresponding percentages of abundance is showed in the Figure 5.

365   **3.4. Binding to BOECs and subsequent P4-induced release changed sperm**

366   **proteomic profiles**

367   In total, 200 protein molecular species with a mass range between 2 and 20 kDa were

368   detected in spermatozoa from the four experimental groups, among which 137 were

369   differential after paired-wise comparisons (Fig. 3B). As for lipidomics, the highest

370   numbers of differential masses were evidenced when comparing BOEC-P4 with

371   spermatozoa treated by P4 alone (P4 group) and CTRL (104 and 98 differential masses,

372   respectively). Comparing with the CTRL group, the P4 group and spermatozoa unbound

373   after incubation with BOECs (BOEC group) displayed 62 and 34 differential masses,

374   respectively. The BOEC-P4 group displayed specific changes in 11 and 14 masses when

375   compared with CTRL and P4, respectively (Fig. 3B). As for lipidomics, the clustering

376   of differential proteins evidenced common changes between the BOEC-P4 and BOEC

377   groups as compared with the CTRL and P4 groups, which also shared similar features

378   (Fig. 4B).

379   **3.5. Identification of differentially abundant proteins**

380   As presented in Supplementary Table 2, a total of 36 *m/z* were identified as fragments

381   of 32 proteins (AKAP4, CALM, ODF2 and SPESP1 were identified by two peptides).

382   In addition, 5 m/z were identified as fragments originated from 2 or 3 different proteins.

Among the proteins identified, five of them (ODF2, ODF3, Sp17, SPAM1 and SPESP1) corresponded to fragments of sperm-specific proteins and nine were found to be altered specifically in the comparison between CTRL and BOEC-P4 (Acrosin, NDUFA6, PHB2, Sp17, ODF2, TPPP2, TUBA3C, OTOF and HDAC9). The known location of the identified proteins included the sperm surface (SPAM1, SPA17), flagellum (ODFs, AKAP4, several subunits of tubulin such as TUBB4B), mitochondria (COX6A1, ACO2, MDH2, PHB2), the equatorial segment (SPES1), nucleus (CLP1, HDAC9, DCAKD) and acrosome (PKM). In addition, according to the Lipid raft proteome database for mammals, prohibitin-2 (PHB2) and tubulin beta 4B-chain (TUBB4B) were found to play roles in lipid rafts.

4. Discussion

The exact mechanism by which spermatozoa detach from the sperm reservoir and the consequences of cell release on sperm physiology are still poorly understood. The main findings of the present work were that spermatozoa released from bovine oviduct epithelial cells by the action of P4 displayed a decrease in the abundance of BSP-3 and -5, an increased membrane fluidity and a number of changes in sperm phospholipids and proteins with a range of biological functions.

The model of BOEC monolayers used in this study was previously shown to display epithelial cell markers such as cytokeratin (Van Langendonckt et al., 1995) and improve early bovine embryo development rate and quality despite partial dedifferentiation during culture (Cordova et al., 2014; Schmaltz-Panneau et al., 2014). Although partially dedifferentiated, BOECs monolayers allowed a reliable and reproducible counting of bound sperm cells in several previous studies (Gualtieri and Talevi, 2003; Lamy et al., 2017; Osycka-Salut et al., 2017; Talevi and Gualtieri, 2001).

407 It is of note that the functional sperm reservoir is located in the distal part of the

408 oviduct, namely the isthmus (Sostaric et al., 2008), while we used BOECs from the

409 complete oviduct. Bovine spermatozoa were reported to interact with OECs from both

410 the ampulla and isthmus but with different dynamics (Ardon et al., 2016). A previous

411 study also demonstrated that sperm-binding capacity of porcine oviductal cells cultured

412 in an air-liquid interphase changed according to the hormonal environment (Chen et al.,

413 2013). Further studies using more physiological BOEC models are needed to evaluate if

414 the P4 action on bound sperm differ according to the oviductal region and mimicked

415 estrous cycle stage.

416 Although sperm capacitation may start immediately after ejaculation *in vivo*, a

417 majority of studies suggest that capacitation of spermatozoa occurs mainly in the

418 oviduct (Holt and Fazeli, 2010; Killian, 2004; Rodriguez-Martinez and Barth, 2007). It

419 is of note that the medium in which sperm incubations were undertaken contained

420 bicarbonate and serum albumin, both reported to be involved in the sperm capacitation

421 process (Aitken and Nixon, 2013). Furthermore, the spermatozoa used were frozen-

422 thawed, a process that could affect biochemical pathways involved in modulating sperm

423 function and in part related to capacitation (Cormier and Bailey, 2003). Therefore, the

424 control group in the present study cannot be considered *sensu stricto* as a 'non-

425 capacitated' group. Spermatozoa in the BOEC group were in vicinity with BOEC

426 without establishing a stable binding after 30 min of co-incubation, including free

427 spermatozoa in the medium, spermatozoa slightly attached to BOEC, or attached and

428 then spontaneously detached from BOEC during incubation. Finally, our study design

429 allowed to study the changes induced by co-incubation with BOEC without P4 action

430 (BOEC group), by P4 alone without stable BOEC binding (P4 group), and finally by the

431 sequential binding to BOEC then P4-induced release (BOEC-P4 group).

432   Binder of Sperm Proteins (BSP) -1, -3 and -5 are a family of proteins from the

433 seminal plasma playing major roles, among others, in the binding of spermatozoa to the

434 oviductal epithelium (Plante et al., 2016a). Immediately after ejaculation, spermatozoa

435 are coated with BSPs, which bind directly to the choline-containing phospholipids such

436 as phosphatidylcholines and sphingomyelins in the sperm membrane (Divyashree and

437 Roy, 2018; Plante et al., 2016b). In the present study, a sharp decrease in the abundance

438 of BSP-3 and -5 was evidenced on spermatozoa bound to BOECs and then released by

439 P4 (BOEC-P4 spz) compared with controls, while BSP-1 tended to decrease in the same

440 group. In accordance, BSPs were found to be lost on bovine spermatozoa after heparin-

441 induced capacitation by other authors (Chiu et al., 2013; Gwathmey et al., 2003). It is

442 likely that in our conditions, the loss of BSPs at the sperm surface was one of the

443 mechanisms by which spermatozoa detach from the BOECs. In parallel with the decline

444 of BSPs on BOEC-P4 spermatozoa, an increase in sperm membrane fluidity and

445 significant changes in the phospholipid profiling were evidenced, highlighting the

446 interaction of BSPs proteins with the phospholipids of the sperm membrane. Indeed,

447 BSP-1 and BSP-3 bind specifically to phospholipids containing the phosphorylcholine

448 group, while BSP-5 binds preferentially to phospholipids containing the

449 phoshorylcholine moiety and to phosphotidylethanolamine, phosphatidylserine,

450 phosphatidylinositol, phosphatidic acid and cardiolipin (Desnoyers and Manjunath,

451 1992). In this way, the loss of BSPs after the sperm release from the BOECs may cause

452 a destabilization of the membrane phospholipids. We performed some FRAP

453 experiments using the sensitive dye DilC12(3), a lipophilic carbocyanine that

454 incorporates into membranes and diffuses laterally within them, resulting in the staining

455 of the entire cell. The advantages of using this staining is that it has an extremely high

456 extinction coefficient and short excited-state lifetime in lipid environments, allowing to

457 distinguish the live cells against the death ones (in contrast with other stainings like

458 Merocyanine 540). Taken together, these results strongly suggest that the detachment of

459 BSPs from the sperm membrane at the time of P4-induced release triggered somehow

460 the remodeling of sperm membrane lipids and finally lead to an increase in sperm

461 membrane fluidity, a process related to sperm capacitation.

462   To our knowledge, this is the first study exploring the lipidomic and proteomic

463 consequences of P4 alone and P4 action after attachment of sperm cells to BOECs. By

464 lipidomics, 34 masses were found differential when comparing BOEC-P4 with CTRL

465 spermatozoa while the treatment by P4 alone did not induce any change in sperm

466 lipidomics. Of interest, the highest number of differential masses (116 masses) was

467 evidenced by comparing the BOEC-P4 group with the P4 group. These results may

468 suggest that the action exerted by P4 on sperm phospholipids modifications is strongly

469 linked to their preliminary binding to BOECs. Probably, the binding to BOECs

470 modified the sperm ability to respond to P4 action or to activate P4-dependent pathways

471 that lead to the remodeling of sperm membranes. Among these differential masses, we

472 could identify 84 lipids. Most of them corresponded to phosphatidylcholines (PC) and

473 sphingomyelins (SM), reaching fold changes of up to 18.5 for PC(36:1) and 8.8 in the

474 case of SM(d40:1) when confronting the BOEC-P4 and CTRL sperm groups. These

475 findings highlight the high impact of P4-induced release on sperm phospholipid

476 composition. A positive association between the increased abundance of several

477 phospholipids and sperm motility was evidenced in equine spermatozoa after thawing

478 (Cabrera et al., 2018). Of interest, five of those phospholipids (PC(34:1), SM(38:1),

479 PC(38:4), PC(35:1) and PC(40:7)) were also identified in the present study as being

480 upregulated in the BOEC-P4 group of spermatozoa compared with P4 and CTRL

481 groups. As BOEC-P4 spermatozoa were previously shown to have an increased

482   fertilizing competence (Lamy et al., 2017), further studies could explore the potential of

483   the differential PC and SM evidenced in this study as biomarkers of the sperm

484   fertilizing ability in the bovine.

485   Sperm lipid rafts are dynamic membrane microdomains enriched with

486   phospholipids, glycosphingolipids and cholesterol, and known to be involved in cell

487   adhesion (Khalil et al., 2006). In addition, lipid rafts contain signaling proteins

488   responsible for various intracellular functions and pathway activation during the sperm

489   capacitation process (Kawano et al., 2011). By using a bovine mammalian lipid raft

490   proteome database, two proteins related to lipid rafts were evidenced among differential

491   proteins: prohibitin-2 (PHB2) and tubulin-β chain 4 (TUBB4B). PHB2 is a membrane

492   protein linked to the mitochondria and shown to act as a chaperone involved in protein

493   and lipid membrane scaffolds (Leonhard et al., 2000). Our results in the present work

494   show a five-fold decrease in PHB2 abundance in the P4 group (ratio of 0.2) but only a

495   two-fold decrease in the BOEC-P4 group (BOEC-P4:CTRL ratio of 0.54) compared

496   with controls. In our opinion these results are quite interesting, since PHB2 is known to

497   be involved in mitochondrial activity (Chai et al., 2017) but also in steroid hormone

498   signaling, functioning as an estrogen receptor (ER)-selective coregulatory factor and

499   able to potentiate the inhibitory activities of antiestrogens and repress the activity of

500   estrogens (He et al., 2008). Therefore, although a similar interaction between PHB2 and

501   PR-related pathway is currently not known, our results suggest a possible role in

502   steroid-related signal transduction of PHB2 during capacitation.

503   By proteomics, a total of 137 differential masses were found between the

504   different sperm groups, among which the highest proportion (98 masses) corresponded

505   to the BOEC-P4 vs. CTRL comparison. This high proportion of masses confirms the

506   strong effect resulting from the combination of sperm attachment to BOECs and

507 subsequent release induced by P4 on sperm physiology. Interestingly, 34 protein masses

508 and 33 lipid masses were found differentially abundant between the BOEC and CTRL

509 groups. Since a high proportion of these differential masses was shared when comparing

510 BOEC-P4 vs. CTRL groups, we consider that these findings may illustrate the existence

511 of a "BOECs effect", by which short periods of sperm binding to and release from the

512 cells could induce molecular changes, although further experiments should be

513 conducted to decipher the exact changes and mechanisms.

514   Among the differential proteins, those with the highest fold-changes in the

515 BOEC-P4 vs. CTRL comparison were flagellar proteins: the A-Kinase anchoring

516 protein 4 (AKAP4; BOEC-P4:CTRL ratio of 4.2) and dynein heavy chain 7 (DNAH7;

517 ratio of 3.6), both more abundant in the BOEC-P4 and in the BOEC groups compared

518 with controls (BOEC:CTRL ratios of 2.7 and 2.8, respectively). AKAP4 and DNAH7

519 are major components of the sperm fibrous sheath (*i.e.* the extent of the principal piece

520 region of the sperm flagellum) that plays important roles in sperm motility (Baccetti et

521 al., 2005; Moretti et al., 2007). Furthermore, AKAP-4 is involved in the cAMP/PKA

522 and PKC/ERK1-2 signaling pathways leading to tyrosine phosphorylation, actin

523 polymerization and acquisition of sperm motility (Rahamim Ben-Navi et al., 2016).

524 AKAP-4 is the mature form obtained from pro-AKAP-4 after the removal of 188 amino

525 acids from the N-terminal domain, which allows AKAP-4 to bind AKAP-3 by the C-

526 terminal domain. In the present study, one of the AKAP-4 peptide (of 4960.6 Da) that

527 was found to be more abundant in the BOEC-P4 group compared with controls

528 corresponds to this C-terminal region of AKAP-4. These results are concordant with

529 those found by others authors (Romero-Aguirregomezcorta et al., 2019), showing an

530 increase in sperm hypermotility at the time of the sperm release from BOECs by the

531 action of P4.

532   DNAH7 is another functional component of sperm motility that was upregulated

533   in BOEC-P4 spermatozoa. Specifically, the corresponding *m/z* was identified as a

534   fragment from the carboxy-terminal region of the dynein heavy chain (DNAH7), which

535   possesses all the elements necessary to produce movement with the energy from the

536   ATP hydrolysis (Roberts et al., 2013). Dyneins are cytoskeletal proteins anchored to the

537   sperm outer microtubules held responsible for generating the force required to produce

538   the beating pattern of the flagellum (Castaneda et al., 2017; Gibbons and Rowe, 1965).

539   Alterations in the gene encoding dynein heavy chain 1 (*DNAH1*) have been shown to

540   cause flagellar abnormalities leading to infertility in some human populations (Sha et

541   al., 2017). Also potentially involved in sperm mobility, fumarate hydratase (FH), an

542   enzyme involved in the Krebs citric acid cycle (Coughlin et al., 1998) and related to

543   ATP production, was found upregulated in BOEC-P4 (ratio of 2.2) spermatozoa

544   compared with controls. This is in agreement with a previous study showing a

545   correlation between down-regulation of major proteins related to ATP production,

546   including FH, and deficiencies of the flagellum in spermatozoa from asthenozoospermic

547   patients (Martinez-Heredia et al., 2008). In summary, BOEC-P4 spermatozoa showed

548   decreased levels of ODF-2 and -3, increased levels of AKAP-4, DNAH7 and FH,

549   proteins related with energy production and sperm motility, and of Sp17, a protein

550   involved in oocyte recognition but also probably in PKA signaling. Taken together, our

551   results are concordant with previous results from our group that reported a higher

552   fertilizing ability of BOEC-P4 spermatozoa (Lamy et al., 2017). However, the ability of

553   those proteins to become biomarkers of male fertility in the bovine remains to be

554   evaluated.

555   **5. Conclusions**

556   In conclusion, P4 at physiological concentrations triggered in vitro the release of

557   a sperm subpopulation characterized by a significant loss of surface BSPs and an

558   increase in membrane fluidity, both events potentially related to capacitation. Moreover,

559   those sperm cells bound to oviduct epithelial cells and then released by P4 presented

560   important changes in phospholipid and protein composition when compared with

561   controls. Our current hypothesis is that P4 acts through progesterone receptors on the

562   sperm membrane to activate specific transduction pathways leading to the selection of a

563   responsive sperm subpopulation with increased fertilizing ability. A number of potential

564   biomarkers of sperm fertility was identified and remain to be validated for application in

565   the field.

566   **Author contributions**

567   MSD and PM conceived the work; all authors curated the data; MSD, MRS, NB

568   and PM performed the formal analysis; NB and PM acquired the funding; MRS

569   performed cell culture experiments; MRS and MCB performed and analyzed FRAP

570   experiments; MRS, VL and XD performed and analyzed mass spectrometry

571   experiments; MRS, GT and XD performed and analyzed Western Blot experiments;

572   MRS created and edited all manuscript figures; NB, PM and MSD administered the

573   project and provided the resources; NB, MSD and PM supervised the work; all authors

574   validated the data; MRS and MSD wrote the original draft with the involvement of all

575   the co-authors; NB and PM critically corrected the draft; all authors reviewed and edited

576   the manuscript; all authors approved the final version of the present manuscript.

577   **Conflict of interest**

578   The authors declare that there is no conflict of interest regarding the publication

579   of this article.

References

Aitken, R.J., Nixon, B., 2013. Sperm capacitation: A distant landscape glimpsed but unexplored. Mol. Hum. Reprod. https://doi.org/10.1093/molehr/gat067

Ardon, F., Markello, R.D., Hu, L., Deutsch, Z.I., Tung, C.-K., Wu, M., Suarez, S.S., 2016. Dynamics of Bovine Sperm Interaction with Epithelium Differ Between Oviductal Isthmus and Ampulla. Biol. Reprod. 95, 90. https://doi.org/10.1095/biolreprod.116.140632

Baccetti, B., Collodel, G., Gambera, L., Moretti, E., Serafini, F., Piomboni, P., 2005. Fluorescence in situ hybridization and molecular studies in infertile men with dysplasia of the fibrous sheath. Fertil. Steril. 84, 123–129. https://doi.org/10.1016/j.fertnstert.2005.01.128

Bernabò, N., Valbonetti, L., Greco, L., Capacchietti, G., Ramal Sanchez, M., Palestini, P., Botto, L., Mattioli, M., Barboni, B., 2017. Aminopurvalanol A, a Potent,

603   Selective, and Cell Permeable Inhibitor of Cyclins/Cdk Complexes, Causes the

604   Reduction of in Vitro Fertilizing Ability of Boar Spermatozoa, by Negatively

605   Affecting the Capacitation-Dependent Actin Polymerization. Front. Physiol. 8,

606   1097. https://doi.org/10.3389/fphys.2017.01097

607   Bertevello, P., Teixeira-Gomes, A.-P., Seyer, A., Vitorino Carvalho, A., Labas, V.,

608   Blache, M.-C., Banliat, C., Cordeiro, L., Duranthon, V., Papillier, P., Maillard, V.,

609   Elis, S., Uzbekova, S., 2018. Lipid Identification and Transcriptional Analysis of

610   Controlling Enzymes in Bovine Ovarian Follicle. Int. J. Mol. Sci. 19, 3261.

611   https://doi.org/10.3390/ijms19103261

612   Blumenthal, D., Goldstien, L., Edidin, M., Gheber, L.A., 2015. Universal Approach to

613   FRAP Analysis of Arbitrary Bleaching Patterns. Sci. Rep. 5, 11655.

614   https://doi.org/10.1038/srep11655

615   Cabrera, T., Ramires-Neto, C., Belaz, K.R.A., Freitas-Dell'aqua, C.P., Zampieri, D.,

616   Tata, A., Eberlin, M.N., Alvarenga, M.A., Souza, F.F., 2018. Influence of

617   spermatozoal lipidomic profile on the cryoresistance of frozen spermatozoa from

618   stallions. Theriogenology 108, 161–166.

619   https://doi.org/10.1016/j.theriogenology.2017.11.025

620   Castaneda, J.M., Hua, R., Miyata, H., Oji, A., Guo, Y., Cheng, Y., Zhou, T., Guo, X.,

621   Cui, Y., Shen, B., Wang, Z., Hu, Z., Zhou, Z., Sha, J., Prunskaite-Hyyrylainen, R.,

622   Yu, Z., Ramirez-Solis, R., Ikawa, M., Matzuk, M.M., Liu, M., 2017. TCTE1 is a

623   conserved component of the dynein regulatory complex and is required for motility

624   and metabolism in mouse spermatozoa. Proc. Natl. Acad. Sci. 114, E5370–E5378.

625   https://doi.org/10.1073/pnas.1621279114

626   Chai, R.-R., Chen, G.-W., Shi, H.-J., O, W.-S., Martin-DeLeon, P.A., Chen, H., 2017.

627   Prohibitin involvement in the generation of mitochondrial superoxide at complex I

628   in human sperm. J. Cell. Mol. Med. 21, 121–129.

629   https://doi.org/10.1111/jcmm.12945

630   Chen, S., Einspanier, R., Schoen, J., 2013. In Vitro Mimicking of Estrous Cycle Stages

631   in Porcine Oviduct Epithelium Cells: Estradiol and Progesterone Regulate

632   Differentiation, Gene Expression, and Cellular Function1. Biol. Reprod. 89.

633   https://doi.org/10.1095/biolreprod.113.108829

634   Chiu, C.-F., Ho, M.-Y., Peng, J.-M., Hung, S.-W., Lee, W.-H., Liang, C.-M., Liang, S.-

635   M., 2013. Raf activation by Ras and promotion of cellular metastasis require

636   phosphorylation of prohibitin in the raft domain of the plasma membrane. Oncogene

637   32, 777–787. https://doi.org/10.1038/onc.2012.86

638   Cordova, A., Perreau, C., Uzbekova, S., Ponsart, C., Locatelli, Y., Mermillod, P., 2014.

639   Development rate and gene expression of IVP bovine embryos cocultured with

640   bovine oviduct epithelial cells at early or late stage of preimplantation development.

641   Theriogenology 81, 1163–1173.

642   https://doi.org/10.1016/J.THERIOGENOLOGY.2014.01.012

643   Cormier, N., Bailey, J.L., 2003. A Differential Mechanism Is Involved During Heparin-

644   and Cryopreservation-Induced Capacitation of Bovine Spermatozoa. Biol. Reprod.

645   69, 177–185. https://doi.org/10.1095/biolreprod.102.011056

646   Coughlin, E.M., Christensen, E., Kunz, P.L., Krishnamoorthy, K.S., Walker, V., Dennis,

647   N.R., Chalmers, R.A., Elpeleg, O.N., Whelan, D., Pollitt, R.J., Ramesh, V., Mandell,

648   R., Shih, V.E., 1998. Molecular Analysis and Prenatal Diagnosis of Human

649   Fumarase Deficiency. Mol. Genet. Metab. 63, 254–262.

650   https://doi.org/10.1006/mgme.1998.2684

651 Coy, P., García-Vázquez, F.A., Visconti, P.E., Avilés, M., 2012. Roles of the oviduct in

652 mammalian fertilization. REPRODUCTION 144, 649–660.

653 https://doi.org/10.1530/REP-12-0279

654 Desnoyers, L., Manjunath, P., 1992. Major proteins of bovine seminal plasma exhibit

655 novel interactions with phospholipid. J. Biol. Chem. 267, 10149–55.

656 Divyashree, B.C., Roy, S.C., 2018. Species-specific and differential expression of BSP-

657 5 and other BSP variants in normozoospermic and asthenozoospermic buffalo (

658 Bubalus bubalis) and cattle (Bos taurus) seminal plasma. Theriogenology 106,

659 279–286. https://doi.org/10.1016/j.theriogenology.2017.10.014

660 Ellington, J.E., Samper, J.C., Jones, A.E., Oliver, S.A., Burnett, K.M., Wright, R.W.,

661 1999. In vitro interactions of cryopreserved stallion spermatozoa and oviduct

662 (uterine tube) epithelial cells or their secretory products. Anim. Reprod. Sci. 56, 51–

663 65.

664 Gibbons, I.R., Rowe, A.J., 1965. Dynein: A Protein with Adenosine Triphosphatase

665 Activity from Cilia. Science (80-.). 149, 424–426.

666 https://doi.org/10.1126/science.149.3682.424

667 Gimeno-Martos, S., González-Arto, M., Casao, A., Gallego, M., Cebrián-Pérez, J.A.,

668 Muiño-Blanco, T., Pérez-Pé, R., 2017. Steroid hormone receptors and direct effects

669 of steroid hormones on ram spermatozoa. Reproduction 154, 469–481.

670 https://doi.org/10.1530/REP-17-0177

671 Gualtieri, R., Talevi, R., 2003. Selection of highly fertilization-competent bovine

672 spermatozoa through adhesion to the Fallopian tube epithelium in vitro.

673 Reproduction 125, 251–8.

674   Gwathmey, T.M., Ignotz, G.G., Mueller, J.L., Manjunath, P., Suarez, S.S., 2006. Bovine

675   Seminal Plasma Proteins PDC-109, BSP-A3, and BSP-30-kDa Share Functional

676   Roles in Storing Sperm in the Oviduct1. Biol. Reprod. 75, 501–507.

677   https://doi.org/10.1095/biolreprod.106.053306

678   Gwathmey, T.M., Ignotz, G.G., Suarez, S.S., 2003. PDC-109 (BSP-A1/A2) Promotes

679   Bull Sperm Binding to Oviductal Epithelium In Vitro and May Be Involved in

680   Forming the Oviductal Sperm Reservoir1. Biol. Reprod. 69, 809–815.

681   https://doi.org/10.1095/biolreprod.102.010827

682   He, B., Feng, Q., Mukherjee, A., Lonard, D.M., DeMayo, F.J., Katzenellenbogen, B.S.,

683   Lydon, J.P., O'Malley, B.W., 2008. A repressive role for prohibitin in estrogen

684   signaling. Mol. Endocrinol. 22, 344–60. https://doi.org/10.1210/me.2007-0400

685   Holt, W. V., Fazeli, A., 2010. The oviduct as a complex mediator of mammalian sperm

686   function and selection. Mol. Reprod. Dev. 77, 934–943.

687   https://doi.org/10.1002/mrd.21234

688   Hunter, R.H., Wilmut, I., 1984. Sperm transport in the cow: peri-ovulatory redistribution

689   of viable cells within the oviduct. Reprod. Nutr. Dev. 24, 597–608.

690   Hunter, R.H.F., 2012. Components of oviduct physiology in eutherian mammals. Biol.

691   Rev. 87, 244–255. https://doi.org/10.1111/j.1469-185X.2011.00196.x

692   Hunter, R.H.F., 2008. Sperm release from oviduct epithelial binding is controlled

693   hormonally by peri-ovulatory graafian follicles. Mol. Reprod. Dev. 75, 167–174.

694   https://doi.org/10.1002/mrd.20776

695   Ito, T., Yoshizaki, N., Tokumoto, T., Ono, H., Yoshimura, T., Tsukada, A., Kansaku, N.,

696   Sasanami, T., 2011. Progesterone Is a Sperm-Releasing Factor from the Sperm-

697   Storage Tubules in Birds. Endocrinology 152, 3952–3962.

698   https://doi.org/10.1210/en.2011-0237

699   Kawano, N., Yoshida, K., Miyado, K., Yoshida, M., 2011. Lipid rafts: keys to sperm

700   maturation, fertilization, and early embryogenesis. J. Lipids 2011, 264706.

701   https://doi.org/10.1155/2011/264706

702   Khalil, M.B., Chakrabandhu, K., Xu, H., Weerachatyanukul, W., Buhr, M., Berger, T.,

703   Carmona, E., Vuong, N., Kumarathasan, P., Wong, P.T.T., Carrier, D., Tanphaichitr,

704   N., 2006. Sperm capacitation induces an increase in lipid rafts having zona pellucida

705   binding ability and containing sulfogalactosylglycerolipid. Dev. Biol. 290, 220–235.

706   https://doi.org/10.1016/j.ydbio.2005.11.030

707   Killian, G.J., 2004. Evidence for the role of oviduct secretions in sperm function,

708   fertilization and embryo development, in: Animal Reproduction Science. pp. 141–

709   153. https://doi.org/10.1016/j.anireprosci.2004.04.028

710   Lamy, J., Corbin, E., Blache, M.-C., Garanina, A.S., Uzbekov, R., Mermillod, P., Saint-

711   Dizier, M., 2017. Steroid hormones regulate sperm–oviduct interactions in the

712   bovine. Reproduction 154, 497–508. https://doi.org/10.1530/REP-17-0328

713   Lamy, J., Liere, P., Pianos, A., Aprahamian, F., Mermillod, P., Saint-Dizier, M., 2016.

714   Steroid hormones in bovine oviductal fluid during the estrous cycle. Theriogenology

715   86, 1409–1420. https://doi.org/10.1016/j.theriogenology.2016.04.086

716   LeDuc, R.D., Fellers, R.T., Early, B.P., Greer, J.B., Thomas, P.M., Kelleher, N.L., 2014.

717   The C-Score: A Bayesian Framework to Sharply Improve Proteoform Scoring in

718   High-Throughput Top Down Proteomics. J. Proteome Res. 13, 3231–3240.

719   https://doi.org/10.1021/pr401277r

720   Leonhard, K., Guiard, B., Pellecchia, G., Tzagoloff, A., Neupert, W., Langer, T., 2000.

721   Membrane protein degradation by AAA proteases in mitochondria: extraction of

722   substrates from either membrane surface. Mol. Cell 5, 629–38.

723   Lukacova, J., Jambor, T., Knazicka, Z., Tvrda, E., Kolesarova, A., Lukac, N., 2015. Dose-

724   and time-dependent effects of bisphenol A on bovine spermatozoa in vitro. J.

725   Environ. Sci. Heal. - Part A Toxic/Hazardous Subst. Environ. Eng. 50, 669–676.

726   https://doi.org/10.1080/10934529.2015.1011963

727   Martinez-Heredia, J., de Mateo, S., Vidal-Taboada, J.M., Ballesca, J.L., Oliva, R., 2008.

728   Identification of proteomic differences in asthenozoospermic sperm samples. Hum.

729   Reprod. 23, 783–791. https://doi.org/10.1093/humrep/den024

730   Mburu, J.N., Rodriguez-Martinez, H., Einarsson, S., 1997. Changes in sperm

731   ultrastructure and localisation in the porcine oviduct around ovulation. Anim.

732   Reprod. Sci. 47, 137–48.

733   Mermillod, P., Vansteenbrugge, A., Wils, C., Mourmeaux, J.L., Massip, A., Dessy, F.,

734   1993. Characterization of the embryotrophic activity of exogenous protein-free

735   oviduct-conditioned medium used in culture of cattle embryos. Biol. Reprod. 49,

736   582–7.

737   Moretti, E., Scapigliati, G., Pascarelli, N.A., Baccetti, B., Collodel, G., 2007. Localization

738   of AKAP4 and tubulin proteins in sperm with reduced motility. Asian J. Androl. 9,

739   641–649. https://doi.org/10.1111/j.1745-7262.2007.00267.x

740   Murray, S.C., Smith, T.T., 1997. Sperm interaction with fallopian tube apical membrane

741   enhances sperm motility and delays capacitation. Fertil. Steril. 68, 351–7.

742   Osycka-Salut, C.E., Castellano, L., Fornes, D., Beltrame, J.S., Alonso, C.A.I.,

743   Jawerbaum, A., Franchi, A., Díaz, E.S., Perez Martinez, S., 2017. Fibronectin From

744   Oviductal Cells Fluctuates During the Estrous Cycle and Contributes to Sperm–

745   Oviduct Interaction in Cattle. J. Cell. Biochem. 118, 4095–4108.

746   https://doi.org/10.1002/jcb.26067

747 Plante, G., Prud'homme, B., Fan, J., Lafleur, M., Manjunath, P., 2016a. Evolution and

748   function of mammalian binder of sperm proteins. Cell Tissue Res. 363, 105–127.

749   https://doi.org/10.1007/s00441-015-2289-2

750 Plante, G., Prud'homme, B., Fan, J., Lafleur, M., Manjunath, P., 2016b. Evolution and

751   function of mammalian binder of sperm proteins. Cell Tissue Res. 363, 105–127.

752   https://doi.org/10.1007/s00441-015-2289-2

753 Rahamim Ben-Navi, L., Almog, T., Yao, Z., Seger, R., Naor, Z., 2016. A-Kinase

754   Anchoring Protein 4 (AKAP4) is an ERK1/2 substrate and a switch molecule

755   between cAMP/PKA and PKC/ERK1/2 in human spermatozoa. Sci. Rep. 6, 37922.

756   https://doi.org/10.1038/srep37922

757 Roberts, A.J., Kon, T., Knight, P.J., Sutoh, K., Burgess, S.A., 2013. Functions and

758   mechanics of dynein motor proteins. Nat. Rev. Mol. Cell Biol. 14, 713–26.

759   https://doi.org/10.1038/nrm3667

760 Rodriguez-Martinez, H., Barth, A.D., 2007. In vitro evaluation of sperm quality related

761   to in vivo function and fertility. Soc. Reprod. Fertil. Suppl. 64, 39–54.

762 Romero-Aguirregomezcorta, J., Cronin, S., Donnellan, E., Fair, S., 2019. Progesterone

763   induces the release of bull spermatozoa from oviductal epithelial cells. Reprod.

764   Fertil. Dev. https://doi.org/10.1071/RD18316

765 Romero-Calvo, I., Ocón, B., Martínez-Moya, P., Suárez, M.D., Zarzuelo, A., Martínez-

766   Augustin, O., de Medina, F.S., 2010. Reversible Ponceau staining as a loading
767   control alternative to actin in Western blots. Anal. Biochem. 401, 318–320.
768   https://doi.org/10.1016/j.ab.2010.02.036

769   Schmaltz-Panneau, B., Jouneau, L., Osteil, P., Tapponnier, Y., Afanassieff, M., Moroldo,
770   M., Jouneau, A., Daniel, N., Archilla, C., Savatier, P., Duranthon, V., 2014.
771   Contrasting transcriptome landscapes of rabbit pluripotent stem cells in vitro and in
772   vivo.   Anim.   Reprod.   Sci.   149,   67–79.
773   https://doi.org/10.1016/j.anireprosci.2014.05.014

774   Sha, Y., Yang, X., Mei, L., Ji, Z., Wang, X., Ding, L., Li, P., Yang, S., 2017. DNAH1
775   gene mutations and their potential association with dysplasia of the sperm fibrous
776   sheath and infertility in the Han Chinese population. Fertil. Steril. 107, 1312-
777   1318.e2. https://doi.org/10.1016/j.fertnstert.2017.04.007

778   Soler, L., Labas, V., Thélie, A., Grasseau, I., Teixeira-Gomes, A.-P., Blesbois, E., 2016.
779   Intact Cell MALDI-TOF MS on Sperm: A Molecular Test For Male Fertility
780   Diagnosis.   Mol.   Cell.   Proteomics   15,   1998–2010.
781   https://doi.org/10.1074/mcp.M116.058289

782   Talevi, R., Gualtieri, R., 2001. Sulfated Glycoconjugates Are Powerful Modulators of
783   Bovine Sperm Adhesion and Release from the Oviductal Epithelium In Vitro1. Biol.
784   Reprod. 64, 491–498. https://doi.org/10.1095/biolreprod64.2.491

785   Teves, M.E., Barbano, F., Guidobaldi, H.A., Sanchez, R., Miska, W., Giojalas, L.C.,
786   2006. Progesterone at the picomolar range is a chemoattractant for mammalian
787   spermatozoa.   Fertil.   Steril.   86,   745–749.
788   https://doi.org/10.1016/j.fertnstert.2006.02.080

789   Therien, I., Manjunath, P., 2003. Effect of Progesterone on Bovine Sperm Capacitation

790   and   Acrosome   Reaction.   Biol.   Reprod.   69,   1408–1415.

791   https://doi.org/10.1095/biolreprod.103.017855

792   Thérien, I., Moreau, R., Manjunath, P., 1999. Bovine seminal plasma phospholipid-

793   binding proteins stimulate phospholipid efflux from epididymal sperm. Biol.

794   Reprod. 61, 590–8.

795   Thérien, I., Moreau, R., Manjunath, P., 1998. Major proteins of bovine seminal plasma

796   and high-density lipoprotein induce cholesterol efflux from epididymal sperm. Biol.

797   Reprod. 59, 768–76.

798   Tienthai, P., 2015. The porcine sperm reservoir in relation to the function of hyaluronan.

799   J. Reprod. Dev. 61, 245–50. https://doi.org/10.1262/jrd.2015-006

800   Van Langendonckt, A., Vansteenbrugge, A., Dessy-Doize, C., Flechon, J.E., Charpigny,

801   G., Mermillod, P., Massip, A., Dessy, F., 1995. Characterization of bovine oviduct

802   epithelial cell monolayers cultured under serum-free conditions. Vitr. Cell. Dev.

803   Biol. - Anim. 31, 664–670. https://doi.org/10.1007/BF02634087

804

805

806   **Figure legends**

807   **Figure 1. Abundance of BSP-1,-3,-5 on sperm cells.** Means ± SEM of

808   normalized values for BSP1, BSP3 and BSP5 (n=3 replicates) quantified by western

809   blot. *$P<0.05$; **$P<0.01$, significance compared with the CTRL group.

810   **Figure 2. Evaluation of sperm membrane fluidity by Fluorescence Recovery**

811   **After Photobleaching** (**FRAP) analysis**. Histogram showing sperm fluidity medians

812   and percentiles 25 and 75% for spermatozoa released by P4 after attachment to BOECs

813   (BOEC-P4) and just manipulated sperm cells (CTRL) Each point represents a sperm

814   cell (n= 6 replicates) *$P<0.05$.

815   **Figure 3. Distribution of differential lipids and proteins in spermatozoa**. A)

816   Venn diagram of all differential masses (m/z, 123 masses in total) from lipidomic

817   analysis among the three comparisons in which differential masses were identified (the

818   CTRL vs. P4 comparison retrieved no difference): CTRL vs. BOEC (33); CTRL vs.

819   BOEC-P4 (34); BOEC-P4 vs. P4 (116); B) Venn diagram of all differential masses

820   (m/z, 151 masses in total) from proteomic analysis among four comparisons between

821   experimental groups: CTRL vs. BOEC (34); CTRL vs. BOEC-P4 (98); CTRL vs. P4

822   (62), BOEC-P4 vs. P4 (104).

823   **Figure 4. Hierarchical clustering of differential lipids and proteins in**

824   **spermatozoa.** A) Heat map representation of differentially abundant lipid masses

825   among experimental groups (CTRL, BOEC, BOEC-P4 and P4); B) Heat map

826   representation of differentially abundant differential protein masses among experimental

827   groups (CTRL, BOEC, BOEC-P4 and P4).

828   **Figure 5. Lipids classification**. Diagram showing the lipids classification

829   including the percentage of each lipid class found after the analysis of lipidomic

830   experiments.

831   **Supplementary Data**

832   **Supplementary Table 1. Identification of lipids detected as differential by**

833   **ICM-MS in bovine spermatozoa.** The MALDI masses (m/z) correspond to the
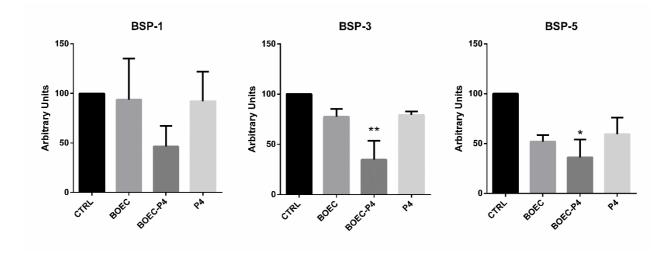
834   observed masses by ICM-MS, confronted to the theoretical mass (Da) and the % of

835   delta mass (<0.1). Fold changes (FC) are ratios of mean normalized intensity values

836   between experimental groups: spermatozoa unbound or released from BOECs after a

837   short period of binding (BOEC), spermatozoa released from BOECs by P4 action

838   (BOEC-P4), treated with P4 without BOECs (P4) or just manipulated (CTRL).

839   **Supplementary Table 2. Identification of proteins detected as differential by**

840   **ICM-MS in bovine spermatozoa**. The MALDI masses (m/z) correspond to the

841   observed masses by ICM-MS, confronted to the theoretical mass (Da) and the % of

842   delta mass (<0.05%). Fold changes (FC) are ratios of mean normalized intensity values

843   between experimental groups: spermatozoa unbound or released from BOECs after a

844   short period of binding (BOEC), spermatozoa released from BOECs by P4 action

845   (BOEC-P4), treated with P4 without BOECs (P4) or just manipulated (CTRL).

Figure 1. Abundance of BSP-1,-3,-5 on sperm cells. Means ± SEM of normalized

values for BSP1, BSP3 and BSP5 quantified by western blot (n=3 replicates). *P<0.05;

**P<0.01, significance compared with the CTRL group.

2-columns fitting image

852

853
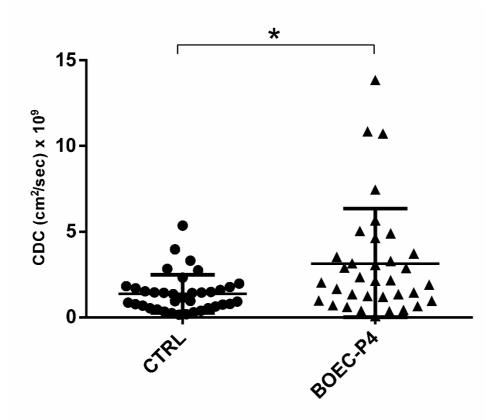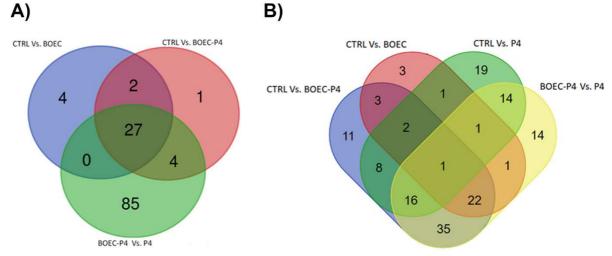
854 **Figure 2. Evaluation of sperm membrane fluidity by Fluorescence Recovery After**

855 **Photobleaching (FRAP) analysis.** Histogram showing sperm fluidity medians and

856 percentiles 25 and 75% for spermatozoa released by P4 after attachment to BOECs

857 (BOEC-P4) and just manipulated sperm cells (CTRL) Each point represents a sperm

858 cell (n= 6 replicates) *P<0.05.

859

860 1-column fitting image

861

Figure 3. Distribution of differential lipids and proteins in spermatozoa. A) Venn

diagram of all differential masses (m/z, 123 masses in total) from lipidomic analysis

among the three comparisons in which differential masses were identified (the CTRL

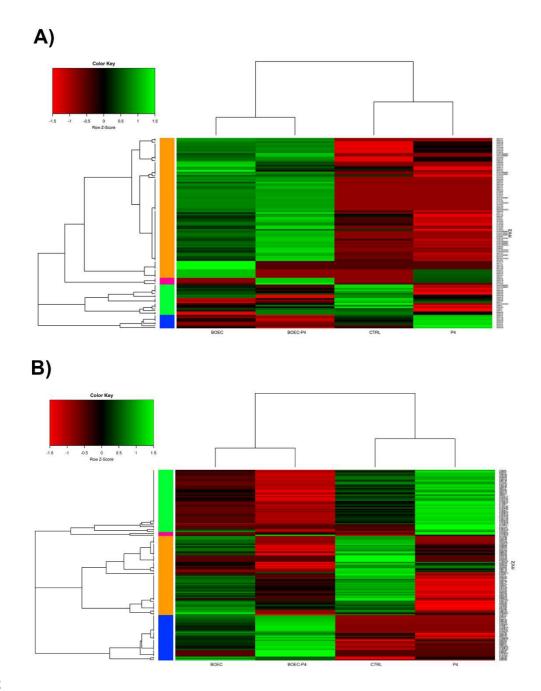vs. P4 comparison retrieved no difference): CTRL vs. BOEC (33); CTRL vs. BOEC-P4

(34); BOEC-P4 vs. P4 (116); B) Venn diagram of all differential masses (m/z, 151

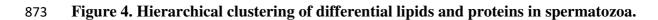masses in total) from proteomic analysis among four comparisons between

experimental groups: CTRL vs. BOEC (34); CTRL vs. BOEC-P4 (98); CTRL vs. P4

(62), BOEC-P4 vs. P4 (104).

870

871   2-columns fitting image

A)

B)

872

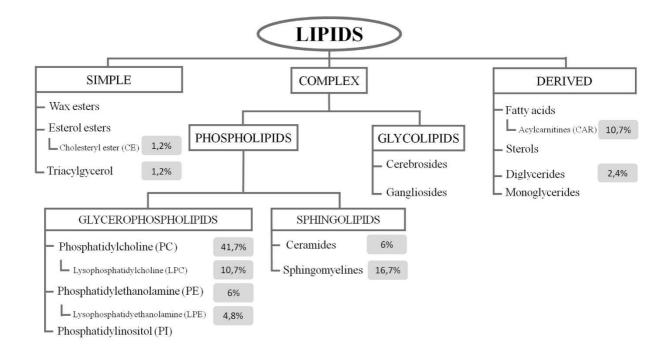**Figure 4. Hierarchical clustering of differential lipids and proteins in spermatozoa.**

A) Heat map representation of differentially abundant lipid masses among experimental

groups (CTRL, BOEC, BOEC-P4 and P4); B) Heat map representation of differentially

abundant differential protein masses among experimental groups (CTRL, BOEC,

BOEC-P4 and P4).

2-columns fitting image

879

880 **Figure 5. Lipids classification**. Diagram showing the lipids classification including the

881 percentage of each lipid class found after the analysis of lipidomic experiments.

882

883 2-columns fitting image